Materials Science

http://www.aimspress.com/journal/Materials

Research article

Electromagnetic interference shielding and thermal properties of non-covalently functionalized reduced graphene oxide/epoxy composites

Suman Chhetri [1,2], Pranab Samanta [1,2], Naresh Chandra Murmu [1,2], Suneel Kumar Srivastava [3], and Tapas Kuila [1,2,]*

[1] Surface Engineering & Tribology Division, Council of Scientific and Industrial Research-Central Mechanical Engineering Research Institute, Durgapur-713209, India

[2] Academy of Scientific and Innovative Research (AcSIR), CSIR-CMERI, Campus, Durgapur-713209, India

[3] Department of Chemistry, Indian Institute of Technology Kharagpur-721302, India

* **Correspondence:** Email: tkuila@gmail.com; Tel: +91-3436510704; Fax: 91-343-2548204.

Abstract: Graphene oxide (GO) was non-covalently functionalized using sulfanilic acid azocromotrop (SAC) followed by hydrazine reduction to achieve SAC functionalized reduced GO (SAC-rGO). Fourier transform infrared spectra analysis and electrical conductivity measurements confirmed the successful functionlization and reduction of GO. The electrical conductivity of ~515 S·m^{-1} for SAC-rGO was recorded. The non-covalently functionalized reduced GO was subsequently dispersed in epoxy matrix at the loading level of 0.3 to 0.5 wt% to investigate its electromagnetic interference (EMI) shielding properties. The morphological and structural characterization of the SAC-rGO/epoxy composites was carried out using X-ray diffraction and Transmission electron microscopy analysis, which revealed the good dispersion of SAC-rGO in the epoxy. The SAC-rGO/epoxy composites showed the EMI shielding of −22.6 dB at the loading of 0.5 wt% SAC-rGO. Dynamical mechanical properties of the composites were studied to establish the reinforcing competency of the SAC-rGO. The storage modulus of the composites was found to increase within the studied temperature. Thermal stability of pure epoxy and its composites were compared by selecting the temperatures at 10 and 50% weight loss, respectively.

Keywords: mechanical property; electromagnetic shielding; thermal stability; glass transition temperature

1. Introduction

In modern era, communication technology and smart electronic devices have become indispensable to human life. However, the advancement in instrumentation has also opened the pandora box for undesirable pollution known as electromagnetic interference (EMI), which is detrimental to the performances and functioning of electronic device, and also to environment and human health. The practice of applying conductive or magnetic materials around the cables, electronics in order to guard them from being malfunction is term as EM shielding (electromagnetic shielding). Effective shielding is essential not only to safeguard the electronic devices, but also equally vital to environment and human health. Therefore, it has become pertinent to devise some shielding mechanism which may mitigate the EM radiation caused by electronic components and protects sensitive circuits and devices from being malfunctioning and degradation. In the past, ample of efforts have been made to develop light weight and radiation absorbing shielding materials. Due to the high electrical conductivity and high permeability, metals have been extensively used as shield [1], as the shield materials must contain free charge carriers in order to interact with the electromagnetic field to abstain the EM radiation. Nevertheless, heavy weight, corrosion vulnerability and difficulties in processing have narrowed the use of metal as EMI shielding materials [2,3]. Of late, polymer composites comprising carbonaceous materials are promulgating significantly against metals and metallic composites materials because of its advantages such as light weight, mechanical flexibility, versatility, easy processability, resistance to corrosion, tunable electrical conductivity and low cost. The uniform dispersion and distribution of filler in the matrix is also crucial to enhance the EMI shielding effectiveness of the composites along with the intrinsic electrical conductivity and aspect ratio of the filler. The higher electrical conductivity and the conductive network of filler can improve EMI shielding properties [4,5,6]. The common conductive filler that have been employed to fabricate conducting composites suitable for EMI shielding applications are carbon nanotubes (CNTs), expandable graphite (EG), grapheme (G), graphene nanoplatelets (GNPs) and carbon nanofibers (CNFs) [7–13]. The unique combination of properties such as high electrical conductivity, large surface area, high mechanical properties and low cost, has facilitated graphene to become one of the potential choice to prepare multifunctional composites.

Graphene oxide (GO), precursor of graphene is crowded with vulnerable oxygen functionalities, which bestow it easy processability and dispersibility in the aqueous media. However, to make graphene compatible with organic solvents, functionlization of its surface by anchoring some organic moiety is crucial. As functionlization not only assist fine dispersion and distribution of graphene in organic polymer, but it also acts as the shield or barrier that restrain single graphene layer from being restacked. Thus, prior to employ in polymer matrix, surface functionlization of graphene is necessary either by covalent or non-covalent technique. Non-covalent functionlization technique preserves the structural integrity of the graphene. The interaction that involved in non-covalent functionlization is π-π interaction, hydrogen bonding and hydrophobic attraction and this technique also preserves the intrinsic chemical structure of graphene [14]. Range of moiety such as surfactants, conjugate aromatic molecule with suitable groups, conjugated polymers have been employed for subtly functionalized the graphene surfaces [15]. Conjugated aromatic molecule with suitable function groups stabilized the graphene through π-π interaction and the pendent group assists to disperse the graphene efficiently in the polymer matrix. Thus, non-covalent modification of GO surface and its subsequent reduction to restore the conjugated π system enable to achieve conducting reduced GO

(rGO), which upon subsequent addition in polymer matrices endow the conductivity to the otherwise insulator polymer.

Herein, sulfanilic acid azo-chromotrop (SAC) has been used to non-covalently functionalize the surface of graphene. It is assumed that SAC molecule is embedded on graphene surface through π-π interaction. The non-covalently functionalized rGO is subsequently dispersed in epoxy to study the EMI shielding and thermomechanical properties. Further, it is also anticipated that the –SO$_3$H groups of SAC interacted with the –OH dipole of epoxy matrix to integrate graphene uniformly into a epoxy matrix, which subsequently improved the interaction and adhesion.

2. Materials and Methods

2.1. Materials

Diglycidyl ether of bisphenol-A based epoxy (Trade name Lapox-B-11) and polyamide hardener composed of long chain fatty acids and triethylenetetramine (Trade name Lapox AH-713) were purchased from Atul Ltd., Gujarat, India. The viscosity of the epoxy resin was 5 Pa·s at 30 °C and its epoxy equivalent weight (EEW) was 185–192 g/eq. The viscosity of the hardener and epoxy/hardener mixture were 21.6 and 20.3 Pa·s, respectively. The number average molecular weight (M_n) of epoxy resin was 374 g/mol. Natural flake graphite was purchased from IndiaMart. Sulphuric acid, hydrogen peroxide, potassium permanganate and N,N-dimethyle formamide (DMF) were obtained from Merck, Mumbai, India. Sulfanilic acid azo cromotrop was purchased from Sigma Aldrich.

2.2. Preparation of Non-covalently Functionalized Graphene

Graphite oxide was prepared through a modied Hummer's method. About 200 mg of graphite oxide dispersed in 200 ml of distilled water by continuous water-bath sonication for ~30 min. The unexfoliated particles was removed by centrifugation at 6000 rpm for 5 minutes and the clear brown dispersion of GO was taken into a 500 ml RB. About 0.6 g of SAC was dissolved in 50 ml of distilled water and added drop wise to the GO dispersion with constant stirring and mixture was stirred at room temperature for ~24 h, afterwards ~1 ml hydrazine monohydrate was added followed by refluxing for ~12 h at 100 °C. The black coloured mixture was cooled to room temperature and washed thoroughly with DI water using a cellulose acetate membrane (pore size 0.1 mm) to remove the unreacted SAC. The black residue thus obtained was dried in a vacuum oven at 60 °C for 3 days and designated as SAC-rGO.

2.3. SAC-rGO/Epoxy Composite Preparation

Different weight fraction of SAC-rGO was dispersed in DMF using water bath sonication for ~1 h. The SAC-rGO dispersion was added into the epoxy resin and the suspension was further sonicated for 1 h. The suspension was heated on a hot plate at ~90 °C with constant stirring at 400 rpm for 5 h to remove excess solvent followed by the removal of residual solvent inside a vacuum oven at ~80 °C for ~16 h. The SAC-rGO/epoxy composites were cooled to room temperature and the hardener was (weight ratio epoxy resin and hardener was 2:1) mixed by high

speed laboratory mechanical mixture at ~1800 rpm for 4 minutes. The composite was then placed inside a degassing chamber for ~30 min to remove air-bubbles and residual solvent. The mixtures was then poured into the silicon mould and cured at room temperature for ~24 h followed by post curing at 80 and 100 ^{o}C for 2 h in each case. Figure 1 shows the schematic of the functionalization of GO with SAC and preparation of its composites with epoxy matrix.
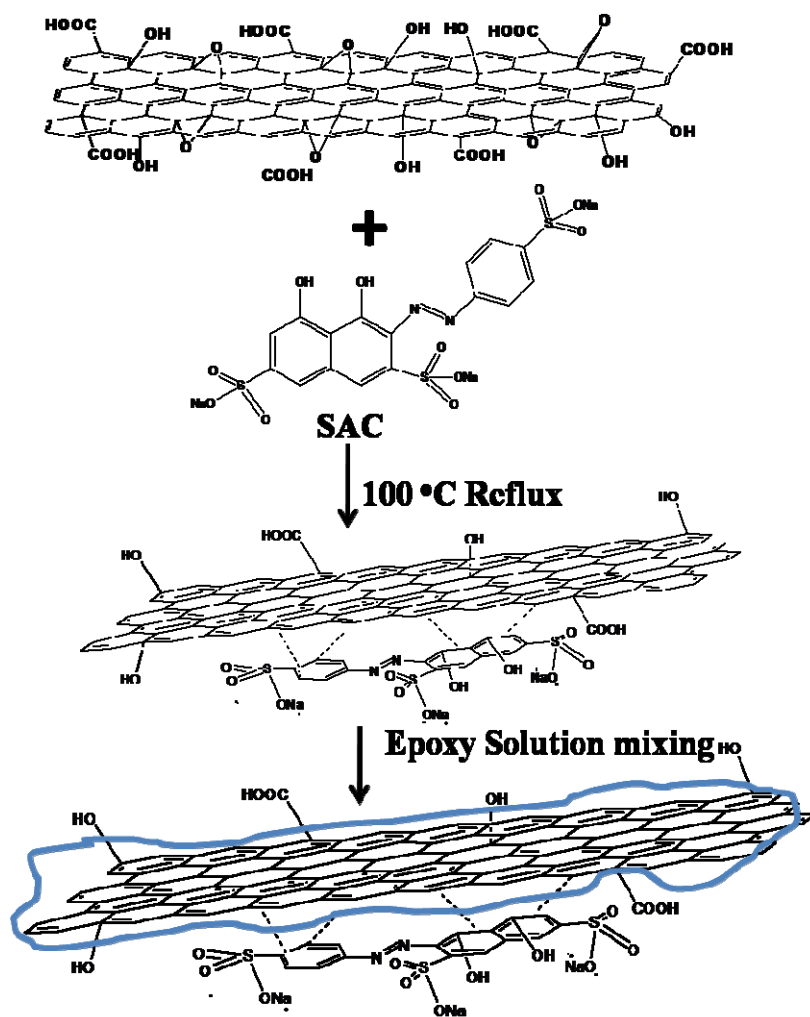

Figure 1. Schematic for the functionalization of GO by SAC and preparation of SAC-rGO/epoxy composites.

2.4. Characterisation

Fourier transform infrared (FT-IR) spectra were recorded with PerkinElmer RXI FT-IR in the frequency range of 4000–400 cm^{-1}. X-ray diffraction (XRD) of GO, SAC-and SAC-rGO/epoxy composites was carried out with PANalytical (Model X pert PRO) at a scan rate of 0.106^{o}·s^{-1} in between the 2θ range of 5–60°. The wavelength of the X-ray beam was λ = 1.5 Å radiations (Cu Kα radiation) operated at 40 kV and 30 mA. Field emission scanning electron microscopy (FE-SEM) was carried out with Σigma HD, Carl Zeiss, India at Central Research Facility of CSIR-CMERI, Durgapur. For Transmission electron microscopy (TEM) observation of SAC-rGO/epoxy composites,

the ultra-thin sample of thickness ~70 nm was cut using Leica Ultracut UCT (Leica EMFCS, USA) ultramicrotome at room temperature. Microtomed SAC-rGO/epoxy samples were collected over copper grids for TEM observation. Dynamic mechanical analysis (DMA) was carried out with DMA 8000 Perkin Elmer in the temperature range of 30 to 160 ^{o}C with a heating rate of 3 ^{o}C·min^{-1} at a constant frequency of 1 Hz at a load strain of 0.010 mm. Rectangular specimens of dimension 10 × 9 × 2.5 mm^{3} were prepared for DMA measurements. Thermogravimetric analysis (TGA) was carried out with Perkin Elmer, Diamond TG/DTA to study the thermal stability of the composites. The samples (~5.56 mg) were heated from 40 to 730 ^{o}C at a heating rate of 5 ^{o}C·min^{-1} under nitrogen atmosphere. EMI shielding efficiency of the SAC-rGO/epoxy composites was performed on the epoxy composites films of thickness 0.1–0.3 mm and diameter 1.5 cm in the frequency range of 100 KHz to 8 GHz by using ENA Series Network Analyzer, E5071C, Agilent Technology. Scattering parameter S$_{21}$ and S$_{11}$ obtained from the analyser was used to calculate the shielding efficiency (SE) parameters. Electrical conductivity (σ) was evaluated by means of a four probe method in a KEITHLEY Delta arrangement consisting of an AC & DC current source, model: 6221 and nanovoltmeter, model: 2182A. The electrical conductivity was calculated according to the following formula [16]

$$conductivity = \frac{1}{4.53 \times \left(\frac{V}{I}\right) \times d} \tag{1}$$

where, I = current in ampere, V = voltage in volt and d is the measured thickness (metre) of the pellet.

3. Result and Discussion

3.1. Electrical Conductivity Analysis

The conversion of brown coloured solution of SAC-GO to black colour aggregates upon the addition of hydrazine hydrate confirmed the reduction of GO. To establish the reduction of GO, electrical conductivity measurement of GO and SAC-rGO was performed. The electrical conductivity of GO was found to be ~6.3 × 10^{-2} S·m^{-1}, while ~515 S·m^{-1} was recorded for SAC-rGO. The enhancement in electrical conductivity value confirms the reduction of GO.

3.2. FT-IR Spectra Analysis

The reduction and non-covalent functionlization of GO were confirmed with FT-IR spectra analysis of GO, SAC and SAC-rGO as shown in Figure 2. The band at 1730 and 1069 cm^{-1} of GO are ascribed to the –C=O stretching vibration of carboxylic and C–O–C in epoxide group, respectively. The peak at 1624 and 1396 cm^{-1} were designated to graphitic sp^{2} C and deformation vibration of the –C–OH group. The peaks associated with oxygen functionalities were absent in the SAC-rGO, which implies the reduction of GO. The band at 1630 cm^{-1} was due to the restoration of C=C bond in rGO. The peak appeared at 1029 cm^{-1} in the spectrum of SAC was attributed to the stretching vibration of –S=O of –SO$_{3}$H. The appearance of peak at 1028 cm^{-1} in the spectrum of SAC-RGO indicates the functionlization of graphene. The diminished in peak intensity and small red shift may be due to the π-π interaction between the SAC and rGO [16].

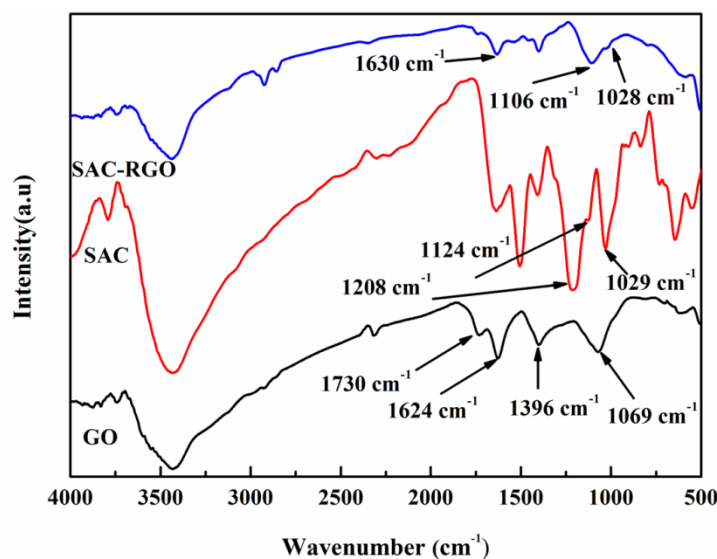**Figure 2.** FT-IR spectra for GO, SAC and SAC-rGO.

3.3. Morphological Analysis

FE-SEM was carried out to study the morphological features of SAC-rGO (Figure 3a & 3b). Figure 3a shows the tightly packed crumpled flaky image of SAC-rGO. It is observed that SAC assist to preserve the layered structure of graphene after being treatment with hydrazine. The wrinkled morphology of graphene is assumed to be helpful in mechanical interlocking with the polymer matrix, which helped in to build strong interfacial interactions and subsequently efficient stress transfer across the interface [17].
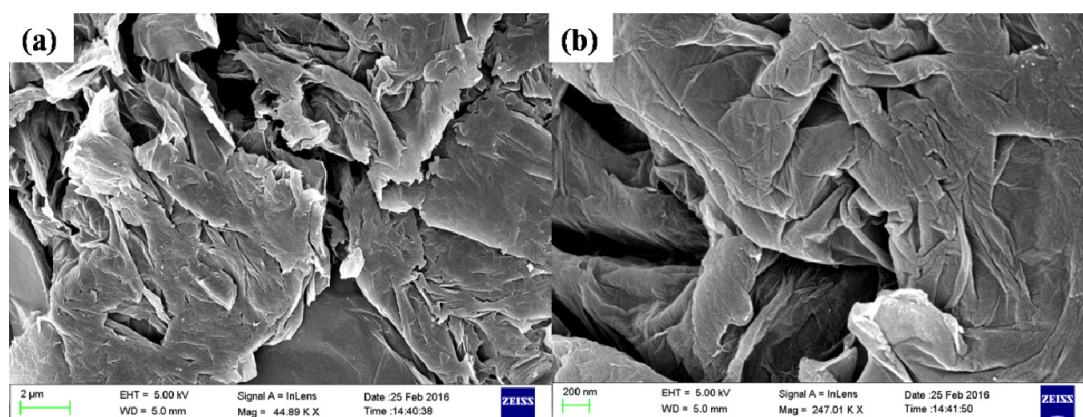

Figure 3. FE-SEM micrographs of SAC-rGO at high and low resolution.

3.4. XRD and TEM Analysis

Figure 4 shows the XRD pattern of pure epoxy and its composites with SAC-rGO. XRD is the helpful tool for accessing the extent of exfoliation of graphene in polymer composites. Normally, the disappearance of characteristic peak for GO sheets in the GO/polymer composites can be correlated

to fully exfoliate GO sheets in the polymer matrix [18–21]. The disappearance of typical diffraction peak of GO and SAC-rGO, indicates the complete exfoliation of graphene in epoxy matrix. Pure epoxy display broad diffraction peak centred at ~18º due to the scattering of cured epoxy molecules, which suggests the amorphous nature of polymer. The composite shows similar diffraction pattern, which could be due to the homogenous dispersion and complete exfoliation of SAC-rGO in the epoxy matrix. To examine the extent of dispersion of SAC-rGO in epoxy matrix, TEM micrograph was recorded with the microtomed sample at the loading of 0.5 wt%. The white portion of the micrograph corresponds to the epoxy matrix and the black regime characterizes to filler particles (Figure 5a and 5b). As it is visible from the images, the SAC-rGO sheets are firmly embedded in the epoxy matrix. Nevertheless, some gaps between filler and epoxy matrix can be viewed in the TEM micrograph, which might be due to the high stress; the diamond knife induces during sample preparation by ultramicrotome [22].
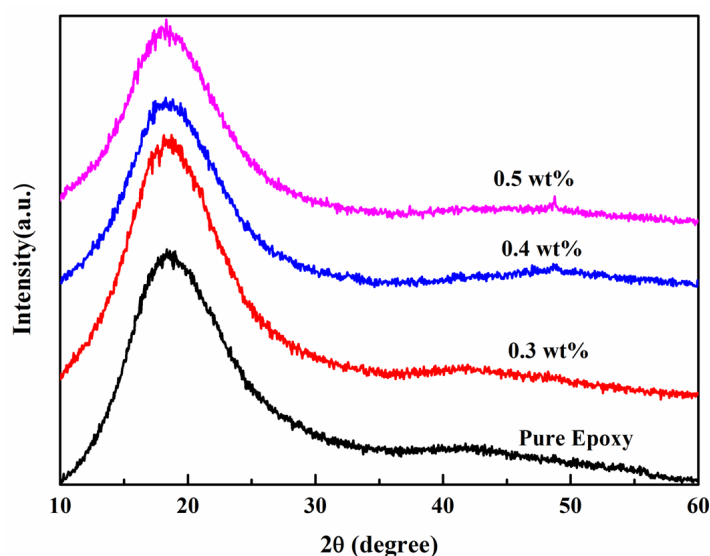

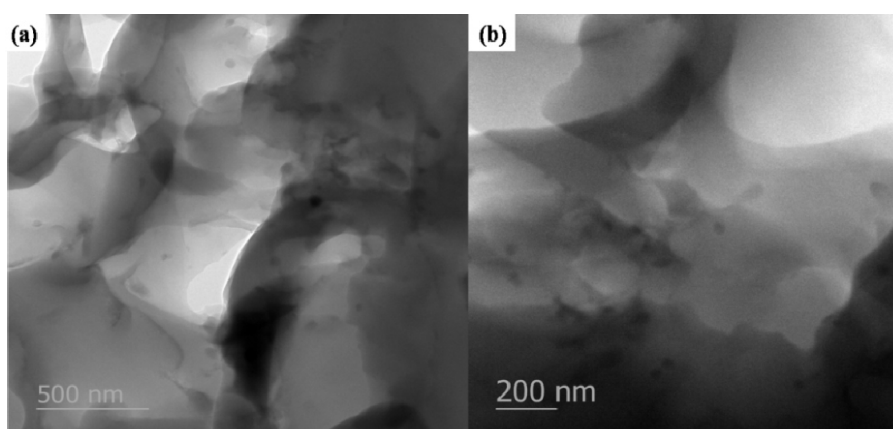**Figure 4.** XRD pattern of SAC-rGO/epoxy composites.

Figure 5. TEM micrograph of SAC-rGO/epoxy composite with 0.3 wt% SAC-rGO at high and low magnification.

3.5. Electromagnetic Interference Shielding Effectiveness (EMI SE)

The EMI SE can be defined as the ability of the shield material to attenuate the electromagnetic field that can be presented as the ratio of incoming (incident) and outgoing (transmitted) power. The total EMI SE of a material is identified to be occurred by the three mechanisms viz; reflection (SE_R), the absorption of electromagnetic energy (SE_A) and the multiple internal reflections (SE_M). The reflection which is considered as the primary mechanism of shielding involves the interactions between the electromagnetic fields and the charge carriers like electron and hole or it can correlate with the impedance mismatch between air and absorber, whereas absorption mechanism is associated with the dielectric/magnetic polarization or energy dissipation [23]. Internal multiple reflections are related with the reflection between the opposite faces of the materials. Therefore, in order to barricade the electromagnetic wave, the shielding material either should absorb or reflect the wave. In general, EMI SE is expressed in decibel (dB) units.

The EMI SE of material can be expressed using the following equation [6,24]:

$$EMI\ SE_{total}(dB) = 10\log\left(\frac{P_I}{P_T}\right) = SE_A + SE_R + SE_M \tag{2}$$

where P_I and P_T are power of incident and transmitted EM waves, respectively. When electromagnetic radiation is incident on the shield material, the summation of power co-efficient of reflectivity (R), absorptivity (A), and transmissivity (T) must be equal to 1, i.e, R + A + T = 1 [25]. When $SE_{total} > 15$ dB, SE_M is supposed to be neglected and the equation can be written as

$$EMI\ SE_{total}(dB) = SE_A + SE_R \tag{3}$$

Treflectivity (R), absorptivity (A), and transmissivity (T) can be deduced from the scattering S parameters obtained from the vector network analyser as follows:

$$T = |S_{12}|^2 = |S_{21}|^2 \tag{4}$$

$$R = |S_{11}|^2 = |S_{22}|^2 \tag{5}$$

$$SE_R = 10log_{10}\left(\frac{1}{1-|S_{11}|^2}\right) \tag{6}$$

$$SE_A = 10log_{10}\left|1 - \frac{|S_{11}|^2}{|S_{12}|^2}\right| \tag{7}$$

$$SE_{total} = 10log_{10}\frac{1}{|S_{12}|^2} = 10log_{10}\frac{1}{|S_{21}|^2} \tag{8}$$

$$A = 1 - T - R \tag{9}$$

The scattering parameters S_{11} and S_{21} are coefficients representing the quantity of electromagnetic reflection and transmission, respectively. Subsequently, we can derive the absorptivity (A), reflectivity (R), and transmissivity (T) using the above equation. The EMI SE of SAC-rGO/epoxy composites was determined in the frequency range of 2–8 GHz (Figure 6). The EMI shielding effectiveness (SE) value of the SAC-rGO/epoxy composites was calculated using equation (8). Pure epoxy is transparent to electromagnetic radiation and do not show any EMI shielding efficiency. With the increase in filler loading, the EMI shielding efficiency of SAC-

rGO/epoxy composites increases. The EMI SE value of 22.6 dB was recorded at 0.5 wt% of SAC-rGO loadings. The EMI SE curves of two composition (0.4 and 0.5 wt%) were found to be merge, nevertheless 0.5 wt% showed little higher EMI SE value (as shown in inset of Figure 6). The high value of EMI SE obtained at low loading of functionalized graphene, can be attributed to the fine dispersion and distribution of conducting SAC-rGO in the polymer matrix, thereby forming interconnected conducting network. Electrical conductivity is very crucial for EMI shielding efficiency, since it is responsible for interacting with the electromagnetic wave. The total EMI SE is influenced by mesh size of the conducting network and the amount of mobile charge carrier provided by the filler network in the composites. The electrical conductivity and the permittivity of the composites are related to the absorption of electromagnetic wave along with the dielectric constant and the thickness of materials. It is anticipated that the conductive network formed by the SAC-rGO interacts with entering power signal and assists the movement of electron within the composites thus responsible for the absorption of incident power. It is also likely that the π-π interaction between the SAC-rGO and epoxy matrix also contributes in movement of electron in the composites. It is expected that the conducting SAC-rGO renders multiple interfaces that increase the reflection and greatly barricade the electromagnetic wave inside the composites. The fine dispersed SAC-rGO particles facilities easy movement of free electron inside the insulating polymer matrix even at low filler loading. The minimum value of EMI SE of the shielding require for practical application is usually considered to be ~20 dB.
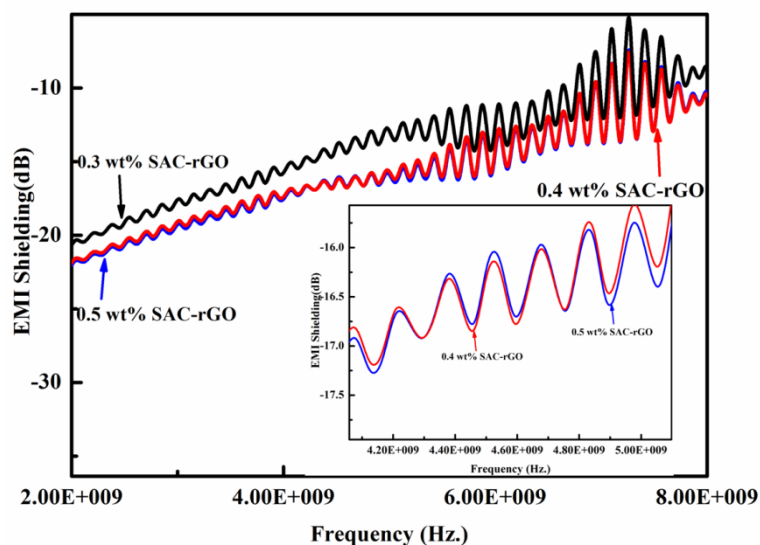

Figure 6. Variation of EMI Shielding Efficiency (EMI SE) against frequency (Hz) of SAC-rGO/epoxy composites at different loading.

3.6. Dynamic Mechanical Analysis

DMA technique renders the information on the storage modulus (E'), loss modulus (E'') and tan δ (E''/E') of the composite materials against temperature. This technique is also helpful to comprehend the degree of interfacial interaction between the polymer matrix and filler. The E' value quantify the elastic behaviour of the material, while E'' compute amount of unrecoverable energy

dissipation per cycle or can also be correlated as the viscous behaviour of the material. The damping parameter or tan δ can be related with the extent of cross-linking density of the polymer and the segmental motion of the polymer chains. Figure 7 represents the DMA plots of E' and tan δ against temperature. Variation in the E' takes place due to the reinforcing effect of the incorporated filler. It can be seen from the E' vs. temperature plot, E' of the composites was found higher than the pure epoxy within glassy region and the highest improvement was recorded for 0.3 wt% composites. The enhancement in the E' can be ascribed to the mechanical restrain imposed by the finely dispersed SAC-rGO particles, which obstruct the segmental motion of the polymer chain. However, small drop in E' was observed on passing through the T_g region. With the increase of the SAC-rGO loading, E' was found to diminish, which may be due to agglomeration of the particles at higher loading.
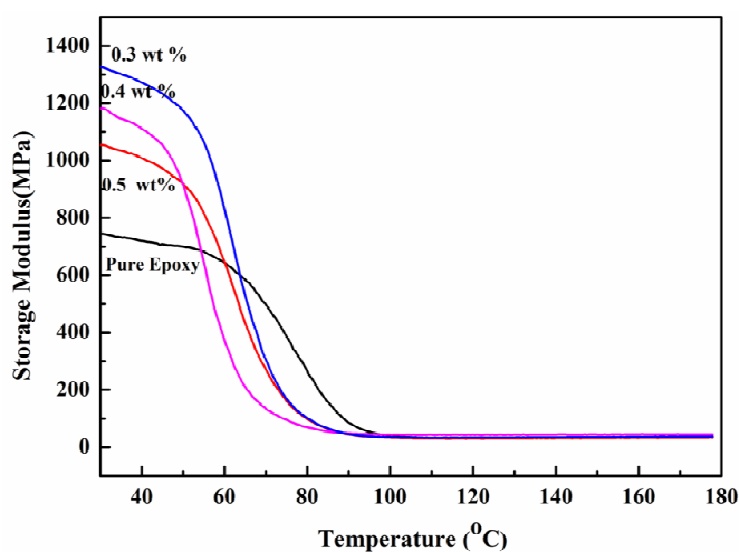

Figure 7. Variation of storage modulus (E') with temperature for SAC-rGO/epoxy composites.

The glass transition temperature (T_g) is derived from the peak position of the tan δ curve. The (T_g) value of the composites was found to decrease against pure epoxy (Figure 8). The T_g value is highly dependent upon the cross-linking density of epoxy. The remaining solvent in the composite perturbs the cross-linking density by altering the stoichiometric ratio of the epoxy and hardener subsequently diminishing T_g value. As high quantity of solvent is required to disperse higher loading of filler, which demand prolong heating to remove the solvent completely, thus probability of reaction between the solvent and epoxy cannot be ruled out, which diminishes the cross linking degree so the T_g value. As DMF solvent was used to disperse the modified graphene, there are the chances that the solvent may interact with the epoxy matrix before removing the solvent. Epoxy molecules on the periphery of DMF solvents now may become unavailable to cross-link with the hardener molecules, which subsequently decreased cross-link density and so T_g value. The lowest T_g value was recorded for 0.5 wt% SAC-rGO/epoxy composites. The increase in free volume around the SAC-rGO aggregates which renders easy movement of uncured epoxy and residual solvent entrapment in the polymer matrix may be other probable reasons for the reduction in T_g. Several

other graphene/epoxy composites have reported the reduction in T_g. Some prior studies of graphene/epoxy composites have reported to diminish Tg value [26,27].
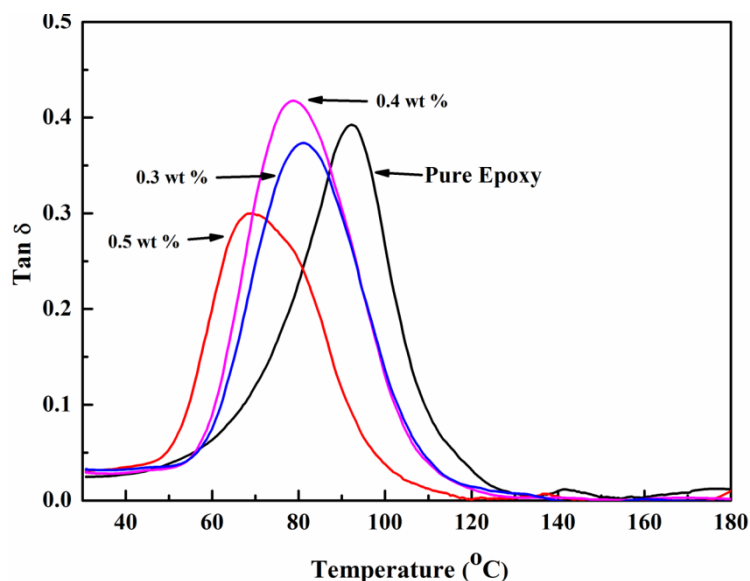

Figure 8. Variation of tan δ with temperature for SAC-rGO/epoxy composites.

3.7. Thermogravimetric Analysis

During its service life, EMI shielding material may subject to high temperature situation, in this study thermal stability of the composites have been analysed. A feasible EMI shield should have suitable thermal stability, so that it may perform well in the elevated temperature. TGA studies were performed to evaluate the thermal degradation properties of pure epoxy and SAC-rGO/epoxy composites. Figure 9a and 9b shows the TGA and DTG curves of the SAC-rGO/epoxy composites The TGA curves show one step degradation mechanism for neat epoxy and its composites with SAC-rGO signifying that the presence of SAC did not significantly change the degradation mechanism of the epoxy matrix. The temperature for 10% ($T_{-10\%}$) and 50% ($T_{-50\%}$) weight loss were selected to examine the thermal stability of the bare epoxy and its composites. The initial degradation temperature of the composites appears to decrease to some extent with increasing the content of SAC-rGO. The small decrease in initial degradation temperature of the composites can be ascribed to the early decomposition of SAC-rGO and the residual solvent traped in the composites. At 50% weight loss, the thermal decomposition temperature of the composites was found to enhance. It may be attributed to the fine dispersion of the SAC-rGO in the polymer matrix, which helped to develop efficient interfacial interaction with the composites. The high aspect ratio of SAC-rGO layered structure may also acted as barrier to prevent the diffusion of small gaseous molecules produced by the thermal degradation. Some prior studies have reported the decrease in degradation temperature of rGO, GO and functionalized graphene epoxy composites [28,29]. Char yield of the cured epoxy composites revealed by the residue weight at 700 ^{o}C was found higher for all the weight fraction against neat epoxy, among which 0.4 wt% of SAC-rGO loading was highest. It could be attributed to optimum dispersion of SAC-rGO in epoxy matrix at 0.4 wt% of SAC-rGO loading resulting in good interfacial interaction, which generated obstruction and impede the volatilization of polymer

decomposition products. The temperature at 10% (T10) and 50% (T50) weight loss and residue percentage are listed Table 1.

DTG curve provides information about the peak temperature, corresponding to that temperature at which maximum weight loss occurred. The main weight loss peak as seen from the DTG curve exhibited similar result for the composites (Figure 9b).
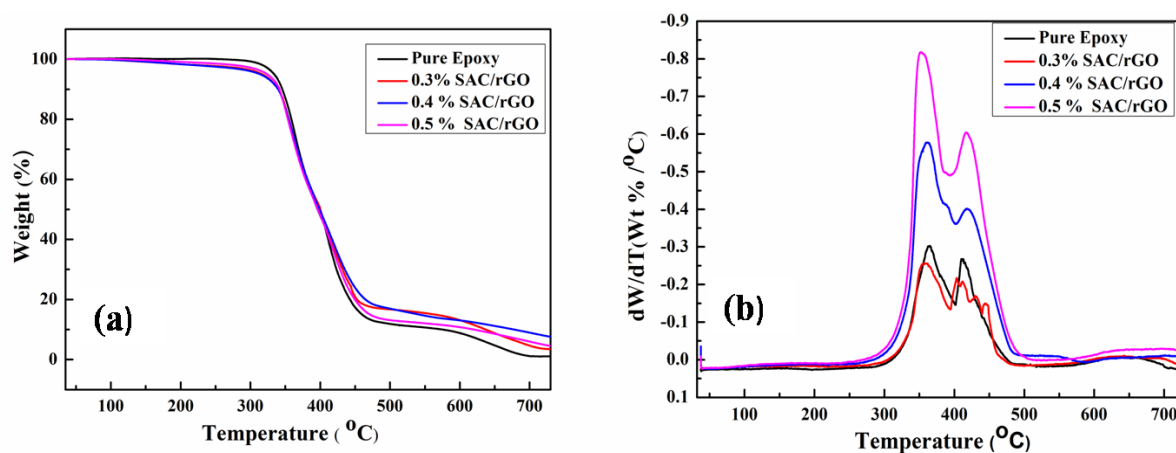

Figure 9. (a) TGA and (b) DTG curves of pure epoxy and SAC-rGO epoxy composites in nitrogen atmosphere.

Table 1. Thermal stability data of the SAC-rGO/epoxy composites obtained from TGA.

Sample	10% weight loss (T_{10})	50% weight loss (T_{50})	Residue (%)
Neat Epoxy	345.6 °C	396.1 °C	1
0.3 SAC-rGO/epoxy	339.6 °C	400.0 °C	4.5
0.4 SAC-rGO/epoxy	339.8 °C	398.5 °C	9
0.5 SAC-rGO/epoxy	341.7 °C	396.5 °C	6.1

4. Conclusions

To exploit the conducting nature of graphene, conducting epoxy composites was fabricated by incorporating non-covalently functionalized reduced graphene oxide. The EMI shielding properties of the so prepared composites was tested and the composites showed the SE value higher than the target value (20 dB). The fine dispersion of high aspect ratio functionalized rGO in the polymer matrix and its electrical conductivity can be attributed for attainment of EMI SE value at such low loading. The improved thermo mechanical properties of the composites revealed the good adhesion between the SAC-rGO and epoxy matrix. TGA studies of the composites were also conducted to study the thermal stability of the composites. In summary, it can be conferred that, if suitably modified the surface of the graphene preserving its conductivity, EMI SE for practical application can be achieved at lower filler loading.

Acknowledgments

Conflict of Interest

The authors declare that there is no conflict of interest regarding the publication of this manuscript.

References

1. Panigrahi R, Srivastava SK (2015) Trapping of Microwave Radiation in Hollow Polypyrrole Microsphere through Enhanced Internal Reflection: A Novel Approach. *Sci Rep* 5: 7638.
2. Kathirgamanathan P (1993) Novel cable shielding materials based on the impregnation of microporous membranes with inherently conducting polymers. *Adv Mater* 5: 281–283.
3. Li P, Du D, Guo L, et al. (2016) Stretchable and conductive polymer films for high-performance electromagnetic interference shielding. *J Mater Chem C* 4: 6525.
4. Chhetri S, Kuila T, Murmu NC (2016) Graphene Composites, In: Nazarpour S, Waite SR, Eds, *Graphene Technology: From Laboratory to Fabrication*, John Wiley & Sons, 63–102.
5. Chen Z, Xu C, Ma C, et al. (2013) Lightweight and Flexible Graphene Foam Composites for High-Performance Electromagnetic Interference Shielding. *Adv Mater* 25: 1296–1300.
6. Li N, Huang Y, Du F, et al. (2006) Electromagnetic Interference (EMI) Shielding of Single-Walled Carbon Nanotube Epoxy Composites. *Nano Lett* 6: 1141–1145.
7. Yang S, Lozano K, Lomeli A, et al. (2005) Electromagnetic interference shielding effectiveness of carbon nanofiber/LCP composites. *Compos Part A-Appl S 36*: 691–697.
8. Farukh M, Dhawan R, Singh BP (2015) Sandwich composites of polyurethane reinforced with poly(3,4-ethylene dioxythiophene)-coated multiwalled carbon nanotubes with exceptional electromagnetic interference shielding properties. *RSC Adv* 5: 75229–75238.
9. Ling J, Zhai W, Feng W, et al. (2013) Facile Preparation of Lightweight Microcellular Polyetherimide/Graphene Composite Foams for Electromagnetic Interference Shielding. *ACS Appl Mater Inter* 5: 2677–2684.
10. Chen Y, Zhang HB, Yang Y, et al. (2016) High-Performance Epoxy Nanocomposites Reinforced with Three-Dimensional Carbon Nanotube Sponge for Electromagnetic Interference Shielding. *Adv Funct Mater* 26: 447–455.
11. Maiti S, Shrivastava NK, Suin S, et al. (2013) Polystyrene/MWCNT/Graphite Nanoplate Nanocomposites: Efficient Electromagnetic Interference Shielding Material through Graphite Nanoplate–MWCNT–Graphite Nanoplate Networking. *ACS Appl Mater Inter* 5: 4712–4724.
12. Liang J, Wang Y, Huang Y, et al. (2009) Electromagnetic interference shielding of graphene/epoxy composites. *Carbon* 47: 922–925.

13. Singh BP, Choudhary V, Saini P, et al. (2012) Designing of epoxy composites reinforced with carbon nanotubes grown carbon fiber fabric for improved electromagnetic interference shielding. *AIP Adv* 2: 022151.

14. Lonkar SP, Deshmukh YS, Abdala AA, et al. (2015) Recent advances in chemical modifications of graphene. *Nano Res* 8: 1039–1074.

15. Kuila T, Bose S, Mishra AK, et al. (2012) Chemical functionalization of graphene and its applications. *Prog Mater Sci* 57: 1061–1105.

16. Jana M, Saha S, Khanra P, et al. (2015) Non-covalent functionalization of reduced graphene oxide using sulfanilic acid azocromotrop and its application as supercapacitor electrode material. *J Mater Chem A* 3: 7323–7331.

17. Du J, Cheng HM (2012) The fabrication, properties, and uses of graphene/polymer composites. *Macromol Chem Phys* 213: 1060−1077.

18. Liang J, Huang Y, Zhang L, et al. (2009) Molecular-Level Dispersion of Graphene into Poly(vinyl alcohol) and Effective Reinforcement of their Nanocomposites. *Adv Funct Mater* 19: 2297−2302.

19. Wang Y, Shi ZX, Fang JH, et al. (2011) Graphene oxide/polybenzimidazole composites fabricated by a solvent-exchange method. *Carbon* 49: 1199−1207.

20. Zaman I, Kuan HC, Meng QS, et al. (2012) A Facile Approach to Chemically Modified Graphene and its Polymer Nanocomposites. *Adv Funct Mater* 22: 2735−2743.

21. Zaman I, Kuan HC, Dai JF, et al. (2012) From carbon nanotubes and silicate layers to graphene platelets for polymer nanocomposites. *Nanoscale* 4: 4578−4586.

22. Tang LC, Wan YJ, Yan D, et al. (2013) The effect of graphene dispersion on the mechanical properties of graphene/epoxy composites. *Carbon* 60: 16–27.

23. Verma P, Saini P, Malik RS, et al. (2015) Excellent electromagnetic interference shielding and mechanical properties of high loading carbon-nanotubes/polymer composites designed using melt recirculation equipped twin-screw extruder. *Carbon* 89: 308–317.

24. Wang JC, Xiang CS, Liu Q, et al. (2008) Ordered Mesoporous Carbon/Fused Silica Composites. *Adv Funct Mater* 18: 2995–3002.

25. Zhang HB, Yan Q, Zheng WG, et al. (2011) Tough Graphene-Polymer Microcellular Foams for Electromagnetic Interference Shielding. *ACS Appl Mater Inter* 3: 918−924.

26. Fang M, Zhen Z, Li J, et al. (2010) Constructing hierarchically structured interphases for strong and tough epoxy nanocomposites by amine-rich graphene surfaces. *J Mater Chem* 20: 9635−9643.

27. Chhetri S, Samanta P, Murmu NC, et al. (2016) Effect of Dodecyal Amine Functionalized Graphene on the Mechanical and Thermal Properties of Epoxy-based Composites. *Polym Eng Sci* [In Press].

28. Jin FL, Ma CJ, Park SJ, et al. (2011) Thermal and mechanical interfacial properties of epoxy composites based on functionalized carbon nanotubes. *Mater Sci Eng A* 528: 8517−8522.

29. Yu G, Wu P (2014) Effect of chemically modified graphene oxide on the phase separation behaviour and properties of an epoxy/polyetherimide binary system. *Polym Chem* 5: 96−104.